

Temporal Evolutions of Electron Density Profiles and its Transport Aspects on LHD

K.Tanaka, K.Kawahata, T.Tokuzawa, S.Okajima¹, A.Ejiri², H.Yamada, O.Kaneko, K.Y.Watanabe, K.Narihara, R.Sakamoto, S.Murakimi, K.Yamazaki, A.Komori, K.Ida, H.Idei, S.Inagaki, S.Kado, S.Kubo, S.Masuzaki, T.Minami, J.Miyazawa, T.Morisaki, S.Morita, T.Mutoh, H.Nakanishi, S.Ohdachi, M.Osakabe, B.J.Peterson, S.Sakakibara, K.Tsumori, O.Motojima, M.Fujiwara and LHD Experiment Group

National Institute for Fusion Science, Toki 509-5292, Japan

¹*Department of Applied Physics, Chubu University, Kasugai 487, Japan*

²*Graduate School of Frontier Sciences, University of Tokyo, Tokyo, 113-0033, Japan*

1. Introduction

The 2nd campaign of LHD experiment was successfully carried out from Sep., 1999 to Dec. 1999 with neutral beam injection (NBI)¹. Good energy confinement characteristics were achieved compared to medium size stellarator scaling². In addition to improvement of the energy confinement, the improvement of the particle confinement is also expected. In this paper, we report the typical electron density profiles of NBI discharges, which are widely varying by the discharge condition (magnetic axis position and particle fueling scheme) and its particle confinement characteristics.

2. Experimental Apparatus and Abel Inversion Scheme

Temporal evolutions of electron density profiles have been measured by the 13 channel vertical view far infrared laser (CO₂ laser pumped CH₃OH laser, wavelength is 118.8 μ m) interferometer³. Figure 1 shows the cross section of the interferometer. The beam width is 40 mm in the plasma, and chord spacing is 90mm. The peripheral chords of interferometer and YAG laser Thomson scattering⁴, which measures electron density from X point to X point in the horizontal view, show the density becomes zero at the outside boundary of the ergodic region, which is shown in fig.1 with a dashed line. Therefore, density contours for the Abel inversion calculation have to be defined in the ergodic region as well. The density contours in the ergodic region are interpolated from the shape of the Last Closed Flux Surfaces (LCFS) and shape of boundary of ergodic region. Contributions of the phase shift caused by the density in the divertor leg are negligible, because the chord at R = 4.3m, which pass through only divertor legs, shows negligible phase shift.

The simple slice and stuck technique are applied for the Abel inversion calculation. Plasma cross section was divided into 10 slices, and average density of each slices are calculated. Then, the radial density profiles are constructed from the averaged density. The boundary of the slices corresponds to magnetic surfaces inside of LCFS, and to interpolated surfaces outside of LCFS. Magnetic flux surfaces are calculated by the MHD equilibrium calculation by using the VMEC code changing the pressure profile and total beta value. Then, the best one is selected to minimize the difference of the radial density profiles between inside and outside of the magnetic axis after trying several magnetic surfaces. As shown in fig. 2, radial density profiles inside

and outside of the magnetic axis have almost same value by using appropriate magnetic surface with magnetic axis shift, however they differ each other by using the vacuum magnetic surface. At high beta (more than 0.5 %) with peaked density profiles, magnetic axis position is well determined by using this scheme. And results have good agreement with iterative MHD equilibrium calculation³.

3. Experimental Results and Discussion

In this section, we concentrate the comparison of two discharges. Both discharges are characterized by the strong density clumping (shot 3560) and weak one (shot 6616). Two discharges are same heating scheme (82.6 and 84 GHz ECRH and 3MW balanced NBI) and different magnetic configurations and toroidal magnetic field (Bt). The magnetic axis position (R_{ax}) of shot 3560 and 6616 were 3.75m and 3.6m respectively. Toroidal magnetic fields (Bt) of shot 3560 and 6616 were 1.5 T and 2.5 T respectively. Both are hydrogen discharges. Figure 3 shows temporal evolutions of line density of shot 3560 (strong density clumping shot). As shown in fig. 3, the line density once drops rapidly at $t = 0.5$ sec although NBI and gas puff are continued, and the density profile changes from flat one (at $t = 0.5$ sec) to hollow one (at $t = 0.8$ sec) as show in fig. 4. In contrast to shot 3560(strong density clumping shot), shot 6616(weak density clumping shot) shows different time history of density profiles. As shown in fig. 5, density clumping occurred at $t = 0.5$ sec as well, but it is small at the central chord, it starts to increase. The density profile changes from hollow one (at $t = 0.5$ sec) to flat one (at $t = 1.0$ sec) as show in fig. 6. In addition, an $H\alpha$ intensity from $t = 0.5$ to 0.8 sec of shot 3560 (strong density clumping shot) are about twice of the one from $t = 0.5$ to 1.0 sec of shot 6616, this indicates particle sources of shot 3560 (strong density clumping shot) are twice of the ones of shot 6616 (weak density clumping shot) during these time periods. This simply suggest shot 6616 (weak density clumping shot) has better particle confinement characteristics than that of shot 3560 (strong density clumping shot). In order to understand the difference of the particle transport quantitatively, correlation of $\text{grad } n_e / n_e$ and Γ / n_e during the shots were examined. Here, Γ is the particle flux, and it can be calculated from the integration form of the

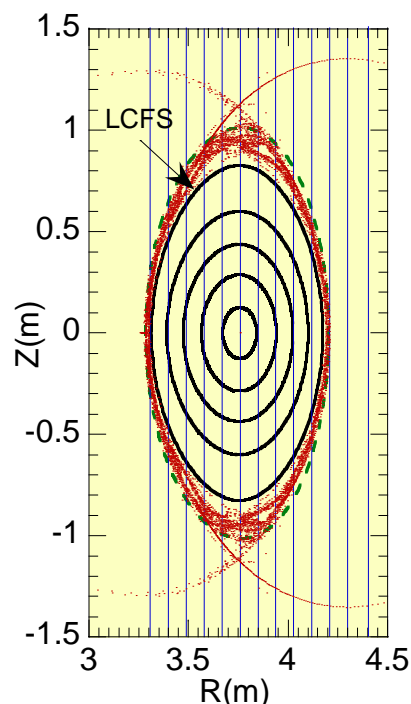


Fig.1 Cross section of multi channel interferometer. Thin blue solid lines indicate interferometer chord. Thick black lines indicate vacuum magnetic surfaces($\rho=0.2, 0.4, 0.6, 0.8, 1.0$) of $R_{ax}=3.75m$. Dots indicate magnetic the field line trace in the ergodic and divertor region.

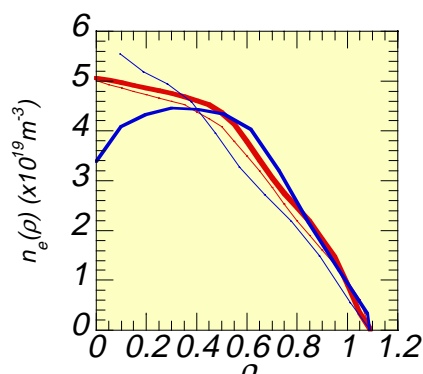


Fig.2 Comparison of Radial density profiles. Shot 6115 $t=0.6$ sec. $\rho=r/a$. r is average radial position, a is average minor radius. Red thick and Red thin lines indicate inner and outer magnetic axis inversion using selected magnetic surfaces respectively. Blue thick and Blue thin lines indicate inner and outer magnetic axis inversion using vacuum magnetic surfaces respectively.

particle balanced equations described by the following.

$$\Gamma(r) = \int_0^r r(S - \frac{\partial n_e}{\partial t}) dr$$

where, S is the source rate, S consists of beam source (S_{NBI}) and wall source (S_{wall}). Radial profiles of S_{NBI} are calculated from 3-D Monte-Carlo simulation chord⁶ and radial profiles of S_{wall} are calculated from 1-D calculation of rate coefficients of dissociative excitation, ionization and dissociative recombination of hydrogen molecules⁷. The absolute values of S_{wall} are calculated assuming particle confinement time is 0.1 sec at $t = 0.5$ sec of shot 3560, which is about same order of the energy confinement time. And temporal factors are multiplied by S_{wall} so that the line integration of calculated S_{wall} are proportional to the measured $H\alpha$ intensity. In fig. 7, the slope of linear line, which can be shown by the following equation, indicates the diffusion coefficients (D) and y-axis intercept indicates the convective velocity (V).

$$\Gamma / n_e = - D \nabla n_e / n_e + V$$

In this analysis, the data of shot 3560 (strong density clumping shot) after $t = 0.8$ sec were excluded, because the density rise during this time period was caused by the increase of impurity accumulation, therefore, determination of the source profiles becomes more complicated. The data of shot 6616 (weak density clumping shot) after $t = 1.0$ sec were also excluded, because change of the wall source condition after turning off the gas puffing might effect on the transport. Data at $\rho=0.7$ were used, because $\text{grad } n_e / n_e$ changes widely in both shots at that radius.

As shown in fig. 7, data of shot 3560 (strong density clumping shot) starts at same data region of shot 6616 (weak density clumping shot), however, transit to different D, V line from that of shot 6616 (weak density clumping shot). In both discharges, during the time period from $t = 0.5$ to $t = 0.6$ sec, electron temperature and its gradient at $\rho = 0.7$ increased rapidly (stronger in shot 3560 (strong density clumping shot)). This could induce outward flux, which is predicted by the neoclassical theory. From this analysis, V is negligible in shot 6616. The better confinement of shot 6616 (weak density clumping shot) can be characterized by smaller V more than smaller D. Although, the analysis is sensitive to the determination of S_{wall} , even if S_{wall} is zero, still shot 3560 (strong clumping shot) needs outward convective velocity (about 0.5 m/sec) to explain the change of density profiles.

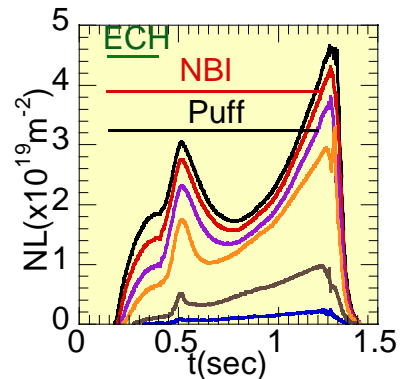


Fig.3 Measured Line density. Shot 3560 $R_{ax}=3.75m, B_t=1.5T$, Hydrogen Plasma 7 ch of 13 ch are shown. Positions of chords are $R=3.759, 3.939, 4.029, 4.209, 4.299, 3.399, 3.309$ (m) from the top.

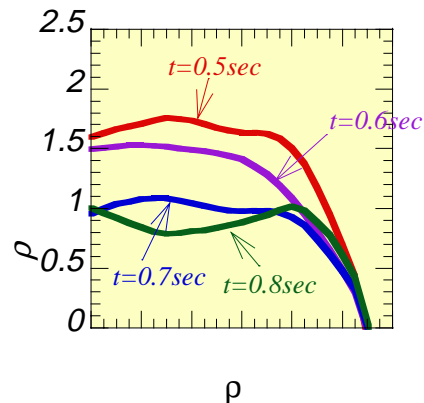


Fig.4 Radial density profiles. Shot 3560 $t = 0.5 \sim 0.8$ sec.

At present, it is not sure whether the difference of the particle confinement between two discharges depends on the difference of R_{ax} or B_t . Experiments and analysis are necessary changing B_t with same R_{ax} , heating scheme and particle source and changing R_{ax} with same B_t , heating scheme and particle source for the further study.

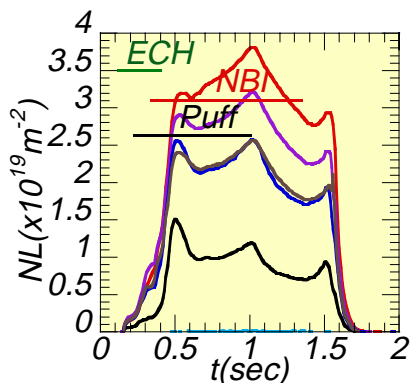


Fig.5 Measured Line density.
Shot 6616 $R_{ax}=3.6m, B_t=2.5T$,
Hydrogen Plasma
Channel positions are same as fig.4.
Data during time periods $t=0.5\sim 1.0$ sec
were used for the analysis in section 3.

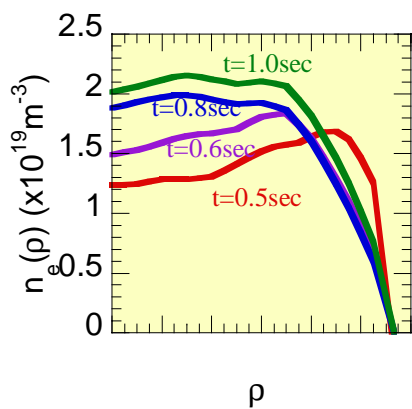


Fig.6 Radial density profiles.
Shot 6616 $t=0.5\sim 1.0$ sec.

References

- [1]O. Motojima et al., Physics of Plasmas Vol.6,No.5, Pt2, p.1843, (1999)
- [2]H.Yamada, et al, this conference
- [3]K.Kawahata,K.Tanaka,Y.Ito A.Ejiri and S.Okajima Rec.Sci, Instrum. 70,1,p.707 ,(1999)
- [4]K.Yamazaki, et al, this conference
- [5]K. Narihara et al. to be published
- [6]S. Murakami, N.Nakajima, and M.Okamoto, Trans. Fusion Tech.27,256 (1995)
- [7] H.C. Howe, ORNL/TM-11521 (1990)

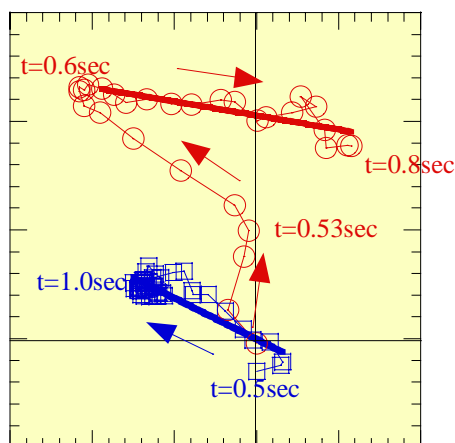


Fig. 7 $1/n_e \frac{dn}{dr} - \Gamma/n_e$ plots

Circles indicate shot 3560 ($R_{ax}=3.75m, B_t=1.5T$) at $\rho=0.7$
from $t=0.5$ to 0.8 sec
Squares indicate shot 6616 ($R_{ax}=3.6m, B_t=2.5T$) at $\rho=0.7$
from $t=0.5$ to 1.0 sec
Data points are every 10 msec.
Positive Γ indicates outward flux.